

# Resonant Einstein-de Haas effect in a rubidium condensate

Krzysztof Gawryluk,<sup>1</sup> Mirosław Brewczyk,<sup>1</sup> Kai Bongs,<sup>2</sup> and Mariusz Gajda<sup>3</sup>

<sup>1</sup> *Instytut Fizyki Teoretycznej, Uniwersytet w Białymstoku, ulica Lipowa 41, 15-424 Białystok, Poland*

<sup>2</sup> *Institut für Laser-Physik, Universität Hamburg, Luruper Chaussee 149, 22761 Hamburg, Germany*

<sup>3</sup> *Instytut Fizyki PAN, Aleja Lotników 32/46, 02-668 Warsaw, Poland*

(Dated: June 25, 2018)

We numerically investigate a condensate of  $^{87}\text{Rb}$  atoms in an  $F = 1$  hyperfine state confined in an optical dipole trap. Assuming the magnetic moments of all atoms are initially aligned along the magnetic field we observe, after the field's direction is reversed, a transfer of atoms to other Zeeman states. Such transfer is allowed by the dipolar interaction which couples the spin and the orbital degrees of freedom. Therefore, the atoms in  $m_F = 0, -1$  states acquire an orbital angular momentum and start to circulate around the center of the trap. This is a realization of the Einstein-de Haas effect in systems of cold gases. We find resonances which amplify this phenomenon making it observable even in very weak dipolar systems. The resonances occur when the Zeeman energy on transfer of atoms to  $m_F = 0$  state is fully converted to the rotational kinetic energy.

Magnetic effects in ultracold quantum gases have been subject to intense theoretical and experimental studies during recent years. So far most of these investigations have concentrated on short-range interactions as the dominant spin exchange process in spinor condensates of  $^{23}\text{Na}$  [1] and  $^{87}\text{Rb}$  [2, 3, 4]. These interactions result in rich multi-component physics as demonstrated by the observation of phenomena like magnetic phases [1, 3, 4], coherent spin dynamics [3, 4, 5, 6], domain formation [7], and a magnetically tuned spin mixing resonance [8]. Including magnetic dipole-dipole interactions would further enhance the richness of these systems and in particular their anisotropic nature is expected to add completely new aspects. Already for relatively weak dipolar interactions phenomena like the Einstein-de Haas effect [9], spontaneous magnetization [10, 11], squeezing and entanglement [11] have been predicted. Most of these studies concentrate on the recently achieved case of a chromium Bose-Einstein condensate [12], as it is commonly believed that these effects are practically unobservable in the widely available alkali condensates due to the smallness of dipolar interactions in these systems. However, as pointed out in [11], for  $^{87}\text{Rb}$  in the  $F = 1$  state the size of the dipolar interactions as compared to the spin-mixing part of the short-range interactions reaches 10%, such that dipolar effects might be observable in this system.

In this Letter, we show that under the right conditions the dipolar interactions can even dominate the dynamics of a  $^{87}\text{Rb}$  spinor condensate, making it a promising candidate for the observation of the Einstein-de Haas effect [13] as an important milestone in dipolar quantum gas physics. In particular our calculations demonstrate the existence of resonances in a spinor rubidium condensate that amplify the effect of dipolar interactions. These resonances can be tuned by the magnetic field or by the trap geometry and occur when the Zeeman energy fits the rotational kinetic energy per particle. The resonances we find explore a new regime in comparison with that considered in Ref. [9] for a  $^{52}\text{Cr}$  condensate, where the dipolar energy (not a kinetic one) is related to the Zeeman

energy.

In the second quantization notation, the Hamiltonian of the system we investigate is given by

$$\begin{aligned} H = & \int d^3r \left[ \hat{\psi}_i^\dagger(\mathbf{r}) \left( -\frac{\hbar^2}{2m} \nabla^2 + U_{ext}(\mathbf{r}) \right) \hat{\psi}_i(\mathbf{r}) \right. \\ & - \gamma \hat{\psi}_i^\dagger(\mathbf{r}) \mathbf{B} \mathbf{F}_{i,j} \hat{\psi}_j(\mathbf{r}) + \frac{c_0}{2} \hat{\psi}_j^\dagger(\mathbf{r}) \hat{\psi}_i^\dagger(\mathbf{r}) \hat{\psi}_i(\mathbf{r}) \hat{\psi}_j(\mathbf{r}) \\ & + \frac{c_2}{2} \hat{\psi}_k^\dagger(\mathbf{r}) \hat{\psi}_i^\dagger(\mathbf{r}) \mathbf{F}_{ij} \mathbf{F}_{kl} \hat{\psi}_j(\mathbf{r}) \hat{\psi}_l(\mathbf{r}) \left. \right] \\ & + \frac{1}{2} \int d^3r d^3r' \hat{\psi}_k^\dagger(\mathbf{r}) \hat{\psi}_i^\dagger(\mathbf{r}') V_{ij,kl}^d(\mathbf{r} - \mathbf{r}') \hat{\psi}_j(\mathbf{r}') \hat{\psi}_l(\mathbf{r}), \end{aligned} \quad (1)$$

where repeated indices (each of them going through the values  $+1, 0$ , and  $-1$ ) are to be summed over. The field operator  $\hat{\psi}_i(\mathbf{r})$  annihilates an atom in the hyperfine state  $|F = 1, i\rangle$  at point  $\mathbf{r}$ . The first term in (1) is the single-particle Hamiltonian ( $H_0$ ) that consists of the kinetic energy part (with  $m$  being the mass of an atom) and the trapping potential  $U_{ext}(\mathbf{r})$ . The second term describes the interaction with the magnetic field  $\mathbf{B}$  with  $\gamma$  being the gyromagnetic coefficient which relates the effective magnetic moment with the hyperfine angular momentum ( $\boldsymbol{\mu} = \gamma \mathbf{F}$ ). The terms with coefficients  $c_0$  and  $c_2$  describe the spin-independent and spin-dependent parts of the contact interactions, respectively –  $c_0$  and  $c_2$  can be expressed with the help of the scattering lengths  $a_0$  and  $a_2$  which determine the collision of atoms in a channel of total spin 0 and 2. One has  $c_0 = 4\pi\hbar^2(a_0 + 2a_2)/3m$  and  $c_2 = 4\pi\hbar^2(a_2 - a_0)/3m$  [14], where  $a_0 = 5.387\text{nm}$  and  $a_2 = 5.313\text{nm}$  [15].  $\mathbf{F}$  are the spin-1 matrices. Finally, the last term describes the magnetic dipolar interactions. The interaction energy of two magnetic dipole moments  $\boldsymbol{\mu}_1$  and  $\boldsymbol{\mu}_2$  positioned at  $\mathbf{r}$  and  $\mathbf{r}'$  equals

$$V_d = \frac{\boldsymbol{\mu}_1 \boldsymbol{\mu}_2}{|\mathbf{r} - \mathbf{r}'|^3} - 3 \frac{[\boldsymbol{\mu}_1(\mathbf{r} - \mathbf{r}')] [\boldsymbol{\mu}_2(\mathbf{r} - \mathbf{r}')] }{|\mathbf{r} - \mathbf{r}'|^5} \quad (2)$$

and since  $\boldsymbol{\mu} = \gamma \mathbf{F}$  one has  $V_{ij,kl}^d(\mathbf{r} - \mathbf{r}') = \gamma^2 \mathbf{F}_{ij} \mathbf{F}_{kl} / |\mathbf{r} - \mathbf{r}'|^3 - 3\gamma^2 [\mathbf{F}_{ij}(\mathbf{r} - \mathbf{r}')] [\mathbf{F}_{kl}(\mathbf{r} - \mathbf{r}')] / |\mathbf{r} - \mathbf{r}'|^5$ .

The equation of motion reads

$$i\hbar \frac{\partial}{\partial t} \begin{pmatrix} \hat{\psi}_1 \\ \hat{\psi}_0 \\ \hat{\psi}_{-1} \end{pmatrix} = (\mathcal{H}_c + \mathcal{H}_d) \begin{pmatrix} \hat{\psi}_1 \\ \hat{\psi}_0 \\ \hat{\psi}_{-1} \end{pmatrix}, \quad (3)$$

where the operator  $\mathcal{H}_c$  originates from the single-particle and two-particle but related to the contact interactions parts of the Hamiltonian (1) whereas  $\mathcal{H}_d$  corresponds to the dipole-dipole interactions. The diagonal part of  $\mathcal{H}_c$  is given by  $\mathcal{H}_{c11} = H_0 + (c_0 + c_2) \hat{\psi}_1^\dagger \hat{\psi}_1 + (c_0 + c_2) \hat{\psi}_0^\dagger \hat{\psi}_0 + (c_0 - c_2) \hat{\psi}_{-1}^\dagger \hat{\psi}_{-1}$ ,  $\mathcal{H}_{c00} = H_0 + (c_0 + c_2) \hat{\psi}_1^\dagger \hat{\psi}_1 + c_0 \hat{\psi}_0^\dagger \hat{\psi}_0 + (c_0 + c_2) \hat{\psi}_{-1}^\dagger \hat{\psi}_{-1}$ ,  $\mathcal{H}_{c-1-1} = H_0 + (c_0 - c_2) \hat{\psi}_1^\dagger \hat{\psi}_1 + (c_0 + c_2) \hat{\psi}_0^\dagger \hat{\psi}_0 + (c_0 + c_2) \hat{\psi}_{-1}^\dagger \hat{\psi}_{-1}$ . The off-diagonal terms that describe the collisions not preserving the projection of spin of each atom (although the total spin projection is conserved) equal  $\mathcal{H}_{c10} = c_2 \hat{\psi}_{-1}^\dagger \hat{\psi}_0$ ,  $\mathcal{H}_{c0-1} = c_2 \hat{\psi}_0^\dagger \hat{\psi}_{-1}$ . Moreover,  $\mathcal{H}_{c1-1} = 0$ . On the other hand, for the  $\mathcal{H}_d$  term one has  $\mathcal{H}_{dij} = \int d^3r' \psi_n^\dagger(\mathbf{r}') V_{ij,nk}^d \psi_k(\mathbf{r}')$ . This term is responsible for the change of total spin projection of colliding atoms. It turns out that when two atoms interact the total spin projection ( $\Delta M_F$ ) can change at most by 2. In particular, the diagonal elements of  $\mathcal{H}_d$  lead to the processes with  $\Delta M_F = \pm 1$ . An example could be the collision of two atoms in  $m_F = 1$  Zeeman state after which one of the atoms goes to the component  $m_F = 0$ . In addition to such processes, the off-diagonal terms of  $\mathcal{H}_d$  introduce the interaction that change the spin projection  $\Delta M_F$  by  $\pm 2$ . It happens when both atoms initially in the same state go simultaneously to the nearest (in a sense of magnetic number  $m_F$ ) state or in the case when atoms in different but neighboring components transfer to the states shifted in number  $m_F$  by  $+1$  or  $-1$ . There is no way for the atom being transferred directly from  $m_F = 1$  to the  $m_F = -1$  state, therefore, the populating of  $m_F = -1$  component is a second order process.

Hence, the dipolar interaction does not conserve the projection of total spin of two interacting atoms. Neither the projection of total orbital angular momentum is preserved (see (4)). However, the dipolar interaction couples the spin and the orbital motion of atoms as revealed by the last relation in (4)

$$\begin{aligned} [V_d, F_{1z} + F_{2z}] &\neq 0, & [V_d, L_{1z} + L_{2z}] &\neq 0, \\ [V_d, L_{1z} + L_{2z} + F_{1z} + F_{2z}] &= 0. \end{aligned} \quad (4)$$

Therefore, going to  $m_F = 0, -1$  states atoms acquire the orbital angular momentum and start to circulate around the center of the trap. This is the realization of the famous Einstein-de Haas effect in cold gases.

To solve the Eq. (3) we neglect the quantum fluctuations and replace the field operator  $\hat{\psi}_i(\mathbf{r})$  by an order parameter  $\psi_i(\mathbf{r})$  for each component and apply the split-operator method. All integrals appearing in  $\mathcal{H}_{dij}$  are the convolutions and we use the Fourier transform technique to calculate them. To find analytical formulas for the Fourier transforms of the components of the convolutions that do not change during the evolution we apply the regularization procedure described in Ref. [16].

The gyromagnetic coefficient for  $^{87}\text{Rb}$  atoms in an  $F = 1$  hyperfine state is positive and equals  $\gamma = \frac{1}{2}\mu_B/\hbar$ . We prepare an initial state of the condensate as the one with all magnetic moments aligned along the magnetic field, i.e., all atoms are in  $m_F = 1$  component. To this end, we run the mean-field version of Eq. (3) in imaginary time while the magnetic field is turned on (and equal to  $B = 0.73 \text{ mG}$  for a spherically symmetric trap with the frequency  $\omega = 2\pi \times 100 \text{ Hz}$ ). Then we reverse the direction of the magnetic field and look for the transfer of atoms to other Zeeman states.

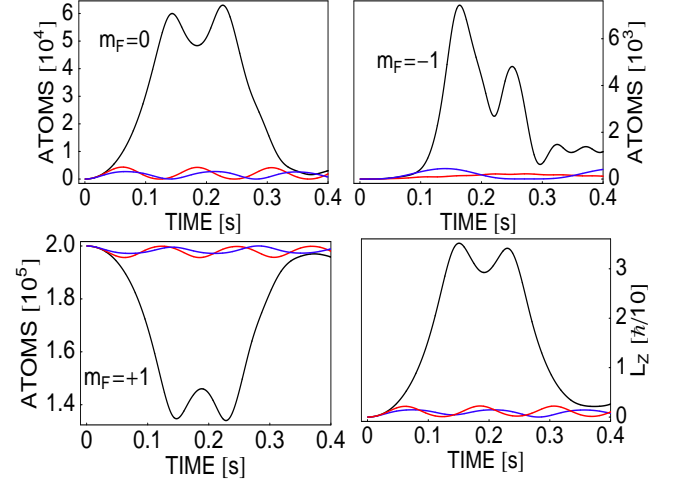


FIG. 1: (color online). Transfer of atoms to  $m_F = 0, -1$  Zeeman states as a function of time. Initially,  $N = 2 \times 10^5$  atoms were prepared in  $m_F = 1$  component in a spherically symmetric trap with the frequency  $\omega = 2\pi \times 100 \text{ Hz}$ . The residual magnetic field equals  $-0.029 \text{ mG}$  (black lines – on-resonance case) and  $B = -0.015 \text{ mG}$ ,  $-0.036 \text{ mG}$  (blue and red lines, respectively – off-resonance case). The lower panel shows: the number of atoms in  $m_F = 1$  state and the time dependence of the orbital angular momentum per atom.

Our starting condition (all atoms in  $m_F = 1$  state) suppresses the short-range spin dynamics and initially the  $m_F = 1$  state is depleted only due to the dipolar interaction. Usually, we observe a small number of atoms going from the Zeeman state  $m_F = 1$  to the  $m_F = 0, -1$  states. However, on resonance (see Fig. 1) the transfer to the other states can be of the order of the initial population of  $m_F = 1$  component. This transfer is as large as in the case of chromium condensate [9] despite the fact that the dipolar energy ( $\mu^2 n$ , where  $n$  is the atomic density) is approximately 100 times smaller. The only difference is that the time scale corresponding to the maximal transfer is about 100 ms, i.e., 100 times longer than for chromium. This can be understood as follows. For  $^{87}\text{Rb}$  the dipolar energy is the smallest energy of the problem and is only a perturbation as compared to the kinetic rotational energy and the Zeeman energy. An efficient population transfer from  $m_F = 1$  to  $m_F = 0$  due to the dipolar interactions is only possible, when the total energies (the sum of mean-field, trap, kinetic, and Zeeman

energies) in these states are approximately equal. Fig. 2a clearly shows that the total energy tends to equalize on resonance, which is not true in the off-resonant case. Numerics also shows (Fig. 2b) that the above condition can be fulfilled only then when the Zeeman energy fits the rotational kinetic energy:  $\mu B_{res} = \epsilon_{rot}$ . It means that the resonant magnetic field is inversely proportional to the magnetic moment of an atom

$$B_{res} \propto 1/\mu. \quad (5)$$

Surprisingly, the smaller atomic magnetic moment the larger value of the resonant magnetic field. For chromium condensate, however, the dipolar energy is larger than the kinetic energy. Therefore, in this case the resonance condition should be derived by relating the Zeeman and the dipolar (not the kinetic one) energies, i.e.,  $\mu B_{res} = \mu^2 n$  [9]. This results in a condition  $B_{res} \propto \mu$  which differs qualitatively from (5).

The maximal transfer is reached at time which is of the order of characteristic time scale determined by the dipolar interactions ( $\hbar/\mu^2 n$ ). Since the magnetic moment of  $^{87}\text{Rb}$  atom is 12 times smaller than that of  $^{52}\text{Cr}$  we have to wait hundreds of milliseconds (not a fraction of millisecond as in Ref. [9]) to see the action of resonance.

Fig. 2 illustrates the ideas just discussed. In the upper frame the total energies of  $m_F = 1, 0$  components are plotted as a function of time both in on- and off-resonance cases showing that the resonances we find is a dynamical phenomenon. The transfer gets maximal when the energies approach each other (perhaps crossing both curves would require the dynamical tuning of the resonance by changing the magnetic field). Contrary, almost no transfer of atoms occurs when the energy curves keep away. Simultaneously, the lower frame proves that on resonance the Zeeman energy (in fact, together with the kinetic energy) is transferred to the rotational kinetic energy of atoms in  $m_F = 0$  component.

Huge transfer of atoms to  $m_F = 0, -1$  states is the realization of the Einstein-de Haas effect in cold gases. Fig. 3a proves that the vortices are generated in  $m_F = 0, -1$  components (though already the lower-right frame in Fig. 1 suggests that atoms in states  $m_F = 0, -1$  rotate around the quantization axis). For  $m_F = 0$  component the phase of the order parameter winds up by  $2\pi$  which means that a singly quantized vortex is formed in this state. At the same time in the  $m_F = -1$  component a doubly quantized vortex is formed (the phase winds up by  $4\pi$ ) as a result of total angular momentum conservation. Fig. 3b shows the typical density patterns in the  $m_F = 0, -1$  states. The density is fragmented and the number of rings in the  $m_F = 0, -1$  components results from the symmetry of dipolar interaction. For example, since the dipolar interaction transforms as a spherical tensor of rank-2 in both spatial and spin spaces, it spatially acts as the spherical harmonic  $Y_{21}$  when atoms go from  $m_F = 1$  to  $m_F = 0$  state. And, since the initial state is spherically symmetric ( $\propto Y_{00}$ ) it induces the spatial behavior  $\propto Y_{21}$  in  $m_F = 0$  component. Therefore, the density in  $m_F = 0$

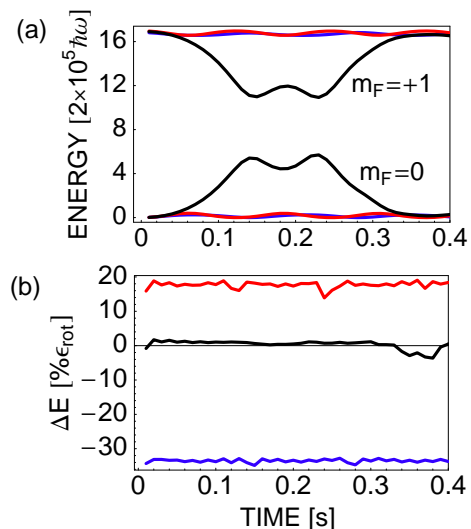


FIG. 2: (color online). Total energy for  $m_F = 1, 0$  components as a function of time (upper frame). All parameters are the same as in Fig. 1. The resonance happens for  $B = -0.029$  mG (black lines) whereas the off-resonance cases are represented by  $B = -0.015$  mG (blue lines) and  $B = -0.036$  mG (red lines). The lower frame shows  $\Delta E = (E_{kin}^{+1}/N_{+1} + \mu B - \epsilon_{rot})/\epsilon_{rot}$ , where  $\epsilon_{rot} = E_{rot}/N_0$ .

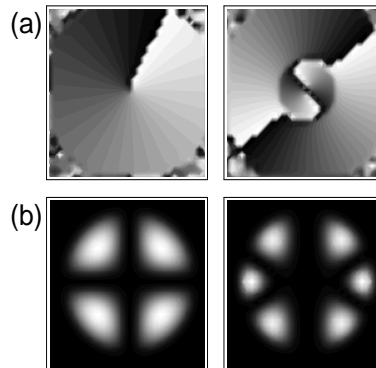


FIG. 3: (a) Phase in the 'xy' plane of  $m_F = 0$  (left frame) and  $m_F = -1$  (right frame) spin components. (b) Density in the 'xz' plane (the 'z' axis goes vertically). All parameters are as in Fig. 1 (on-resonance case) and the density cuts are taken at 140 ms.

state shows two rings. Similar fragmentation was already predicted in the case of  $^{52}\text{Cr}$  condensate in Ref. [9].

Fig. 4 (upper frame) shows the position and the width of the resonance displayed in Fig 1. Similar behavior is observed when the value of the reversed magnetic field is kept constant and the trap geometry is changed (lower frame). Here, the maximal transfer of atoms is obtained in a cigar trap with the aspect ratio  $\omega_\rho/\omega_z = 4$  with almost 50% efficiency at  $B = -0.073$  mG. The inset shows the resonance at experimentally easier to control value of magnetic field  $B = 0.3$  mG but still detectable number of atoms in  $m_F = 0$  state. To un-

derstand quantitatively the resonance we start from the condition discussed earlier:  $\mu B_{res} = E_{rot}/N_0$ , where  $E_{rot}$  is the rotational energy of  $m_F = 0$  component which is assumed to be a singly quantized vortex, given within the Thomas-Fermi approximation by  $\psi_0(\rho, \phi, z) = [(\lambda - m\omega^2(\rho^2 + z^2)/2 - \hbar^2/(2m\rho^2))/c_0]^{1/2} \times e^{i\phi}$ . Here, the chemical potential  $\lambda$  is obtained by the requirement that the number of atoms in  $\psi_0$  state equals  $N_0$ . One can tune to the resonance in two ways: a) by adjusting the magnetic field  $B$ ; b) by changing the trap geometry what influences the rotational energy entering resonance condition and keeping the magnetic field constant. The resulting curve for the spherically symmetric trap is plotted in Fig. 5. The numerical results are marked by balls and correspond to the initial number of atoms in  $m_F = 1$  component equal to  $2 \times 10^5$ ,  $8 \times 10^5$ , and  $2 \times 10^6$  showing a good agreement. For other systems, e.g.  $^{52}\text{Cr}$ , the condition  $\mu B_{res} = E_{rot}/N_{m_F}$  suggests that the value of the resonant magnetic field is even  $\approx 10$  times smaller since  $\mu_{Cr}/\mu_{Rb} = 12$  and  $E_{rot}/N_{-2}$  for chromium looks similar as  $E_{rot}/N_0$  in the rubidium case.

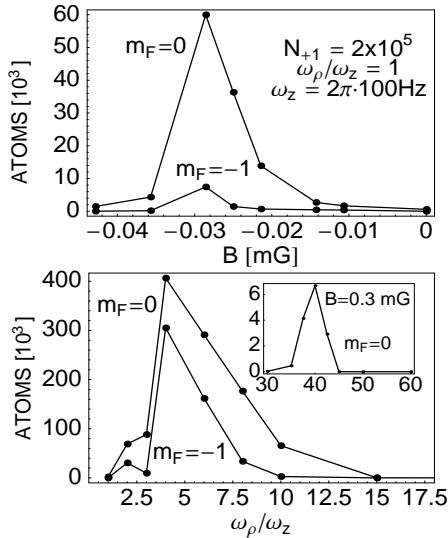


FIG. 4: Maximal transfer of atoms to  $m_F = 0, -1$  states as a function of the residual magnetic field (upper frame) and the trap geometry (lower frame). For lower frame  $\omega_z = 2\pi \times 100$  Hz,  $B = -0.073$  mG, and  $N_{+1} = 8 \times 10^5$ . Inset shows the resonance at  $B = -0.3$  mG for  $\omega_z = 2\pi \times 20$  Hz and  $N_{+1} = 10^5$ .

In conclusion, we have shown the existence of dipolar resonances in rubidium spinor condensates. The resonances occur when the Zeeman energy of atoms in  $m_F = 1$  component, while transferring to  $m_F = 0$  state, is fully converted to the rotational kinetic energy. This is so far an unexplored regime. Symmetries of the dipolar interaction force the atoms in  $m_F = 0, -1$  states to circulate around the quantization axis and form singly and doubly quantized vortices, respectively. Therefore, dipolar resonances is a route to the observation of the Einstein-de Haas effect (as well as other phenomena re-

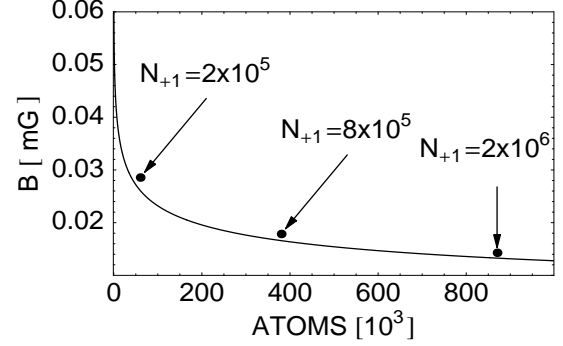


FIG. 5: Comparison between numerics (balls) and the Thomas-Fermi approximation. Solid line indicates the value of the magnetic field at resonance (for spherically symmetric trap) as a function of number of atoms in  $m_F = 0$  state.

lated to the dipolar interaction) in weak dipolar systems.

## Acknowledgments

We are grateful to J. Kronjäger, J. Mostowski, and K. Rzażewski for helpful discussions. M.B. and M.G. acknowledge support by the Polish KBN Grant No. 1 P03B 051 30. K.G. thanks the Polish Ministry of Scientific Research Grant Quantum Information and Quantum Engineering No. PBZ-MIN-008/P03/2003.

- 
- [1] J. Stenger *et al.*, Nature **396**, 345 (1998).
  - [2] M. R. Matthews *et al.*, Phys. Rev. Lett. **81**, 243, (1998).
  - [3] H. Schmaljohann *et al.*, Phys. Rev. Lett. **92**, 040402 (2004).
  - [4] M.-S. Chang *et al.*, Phys. Rev. Lett. **92**, 140403 (2004).
  - [5] M.-S. Chang *et al.*, Nature Physics **1**, 111-116 (2005).
  - [6] J. Kronjäger *et al.*, Phys. Rev. A **72**, 063619 (2005).
  - [7] L. E. Sadler *et al.*, cond-mat/0605351.
  - [8] J. Kronjäger *et al.*, cond-mat/0606046.
  - [9] Y. Kawaguchi, H. Saito, and M. Ueda, Phys. Rev. Lett. **96**, 080405 (2006).
  - [10] R. Cheng, J.-Q. Liang, and Y. Zhang, J. Phys. B: At. Mol. Opt. Phys. **38**, 2569 (2005).
  - [11] S. Yi and H. Pu, Phys. Rev. A **73**, 023602 (2006).
  - [12] L. Santos and T. Pfau, Phys. Rev. Lett. **96**, 190404 (2006).
  - [13] A. Einstein and W. J. de Haas, Verh. Dtsch. Phys. Ges. **17**, 152 (1915).

- [14] T.-L. Ho, Phys. Rev. Lett. **81**, 742 (1998); T. Ohmi and K. Machida, J. Phys. Soc. Jap. **67**, 1822 (1998).
- [15] E. G. M. van Kempen *et al.*, Phys. Rev. Lett. **88**, 093201 (2002).
- [16] K. G3ral and L. Santos, Phys. Rev. A **66**, 023613 (2002).